Journal of Non-Newtonian Fluid Mechanics 197 (2013) 24–30

Contents lists available at SciVerse ScienceDirect

Journal of Non-Newtonian Fluid Mechanics

journal homepage: http://www.elsevier.com/locate/jnnfm

Newtonian Poiseuille flows with slip and non-zero slip yield stress

George Kaoullas [a,*], Georgios C. Georgiou [b]

[a] Oceanography Centre, University of Cyprus, PO Box 20537, 1678 Nicosia, Cyprus
[b] Department of Mathematics and Statistics, University of Cyprus, PO Box 20537, 1678 Nicosia, Cyprus

ARTICLE INFO

Article history:
Received 9 December 2012
Received in revised form 11 February 2013
Accepted 12 February 2013
Available online 6 March 2013

Keywords:
Newtonian fluid
Poiseuille flow
Navier slip
Slip yield stress

ABSTRACT

The Newtonian Poiseuille flow is considered for various geometries, under the assumption that wall slip occurs above a critical value of the wall shear stress known as, the slip yield stress. In the axisymmetric and planar cases, there are two flow regimes defined by a critical value of the pressure gradient above which slip occurs. Two critical pressure gradients characterise the annular and rectangular Poiseuille flows. Below the first critical value no-slip occurs while above the second-one, slip occurs at all walls. In the intermediate regime for the annular problem, slip occurs only at the inner-wall, while for the rectangular problem, there are two intermediate regimes for which there are no analytical solutions. In the first regime slip occurs only in the middle sections of the wider walls and in the second-one partial slip also occurs along the narrower walls. Analytical solutions of all flow problems (with the exception of the two intermediate regimes of the rectangular Poiseuille case) are derived and discussed.

© 2013 Elsevier B.V. All rights reserved.

1. Introduction

Slip at the wall occurs in many industrial applications involving complex fluids, such as suspensions, emulsions, and polymer melts and solutions [1–3]. Newtonian fluids are known to obey the classical no-slip boundary condition of fluid mechanics. However, recent developments concerning biological and engineering devices and systems in microscale which involve fluid flow through microchannels have demonstrated that the no-slip boundary condition is not valid [4]. A number of experiments have shown that under certain conditions slip occurs at the wall [5–7].

Denn [2] notes that according to the experimental data, the slip velocity, i.e. the relative velocity of the fluid with respect to that of the wall, is in general a function of the wall shear stress, the wall normal stress, the temperature, the molecular weight and its distribution, and the fluid/wall interface, e.g. the interaction between the fluid and the solid surface and surface roughness. Navier [8] was the first to propose a slip model stating that the slip velocity is proportional to the wall shear stress:

$$u_w = \frac{\tau_w}{\beta}, \tag{1}$$

where β is the slip coefficient, which varies in general with temperature, normal stress, pressure, molecular parameters, and the characteristics of the fluid/wall interface [2]. As $\beta \to 0$ the-no slip boundary condition is recovered, while for $\beta \to \infty$ one gets perfect slip. The slip coefficient is also defined by

$$\beta \equiv \frac{\eta}{b}, \tag{2}$$

where η is the viscosity and b is the extrapolation length, i.e. the characteristic length equal to the distance that the velocity profile at the wall must be extrapolated to reach zero. Many experimental results (see Refs. [4,9]) provide evidence to support the Navier slip condition. Other slip equations are also used in the literature, the most important of which are the generalisations to power-law and dynamic slip equations [3]. In the present work, we are interested in models allowing slip only above a certain critical value of wall shear stress, τ_c as suggested by experimental data on several fluid systems (see Ref. [10] and references therein). This critical wall shear stress value is called slip yield stress and is similar to a Coulomb friction term. A simple extension of Navier's law to include slip yield stress is the following

$$u_w = \begin{cases} 0, & \tau_w \leqslant \tau_c, \\ \frac{1}{\beta}(\tau_w - \tau_c), & \tau_w > \tau_c. \end{cases} \tag{3}$$

The extension of the above slip equation with the introduction of a power-law exponent is also very often used. Such a slip equation was employed, for example, by Estellé and Lanos [11] in the analysis of squeeze flow of Bingham fluids, and more recently, by Ballesta et al. [12] in their study of slip and flow of concentrated colloidal suspensions.

Analytical solutions of Newtonian Poiseuille flows with Navier slip (i.e. with zero yield stress) have been presented for different geometries such as axisymmetric, planar, annular, and rectangular.

* Corresponding author. Tel.: +357 99478302.
E-mail addresses: g.kaoullas@gmail.com (G. Kaoullas), georgios@ucy.ac.cy (G.C. Georgiou).

0377-0257/$ - see front matter © 2013 Elsevier B.V. All rights reserved.
http://dx.doi.org/10.1016/j.jnnfm.2013.02.005

These include steady-state solutions [13–16], or transient [9,17,18] and periodic [19–21] solutions. Recently, Ferrás et al. [22] presented analytical solutions for both Newtonian and inelastic non-Newtonian fluids with slip boundary conditions in Couette and Poiseuille flows using the Navier linear and non-linear slip laws.

The purpose of this paper is to give analytical results for steady-state, Newtonian Poiseuille flows in the case of slip with non-zero slip yield stress for the annular and rectangular geometries. For completeness the solutions for the axisymmetric and planar Poiseuille flows are first provided in Section 2. In Section 3 we give the steady state solution for the annular Poiseuille flow. In Section 4 solutions for the two-dimensional rectangular problem are given. Finally, in Section 5 the conclusions of this work are provided.

2. Axisymmetric Poiseuille flow

We consider the steady, creeping, pressure-driven flow of an incompressible, Newtonian fluid in a circular tube of radius R under the assumption of zero gravity. The flow is thus unidirectional and, in cylindrical polar coordinates, the z-velocity component satisfies

$$G+\eta\left(\frac{\mathrm{d}^2u_z}{\mathrm{d}r^2}+\frac{1}{r}\frac{\mathrm{d}u_z}{\mathrm{d}r}\right)=0, \tag{4}$$

where $G\equiv(-\partial p/\partial z)$ is the pressure gradient. The wall shear stress is defined as

$$\tau_w=|\tau_{rz}|_{r=R}=-\eta\left.\frac{\mathrm{d}u_z}{\mathrm{d}r}\right|_{r=R}. \tag{5}$$

Thus, from Eq. (3) the boundary condition at the wall is

$$u_w=\begin{cases}0, & \tau_w\leqslant\tau_c,\\ -\frac{1}{\beta}\left(\eta\frac{\mathrm{d}u_z}{\mathrm{d}r}+\tau_c\right), & \tau_w>\tau_c,\end{cases} \tag{6}$$

while symmetry is assumed at the axis of symmetry. It is clear that there are two flow regimes: (i) the no-slip and (ii) the slip regime. The wall shear stress given by

$$\tau_w=\frac{GR}{2}, \tag{7}$$

only depends on the pressure gradient. The critical value of the pressure gradient for the occurrence of slip G_c, is found by setting $\tau_w=\tau_c$. Thus,

$$G_c=\frac{2\tau_c}{R}. \tag{8}$$

It is easily shown that

$$u_z(r)=\begin{cases}\frac{R^2G}{4\eta}\left[1-\left(\frac{r}{R}\right)^2\right], & G\leqslant G_c,\\ \frac{R^2G}{4\eta}\left[1+2B-\left(\frac{r}{R}\right)^2\right]-\frac{\tau_cBR}{\eta}, & G>G_c,\end{cases} \tag{9}$$

where

$$B\equiv\frac{\eta}{\beta R}, \tag{10}$$

is the dimensionless slip number. When $G\leqslant G_c$ the no-slip solution applies and if $G>G_c$ and $\tau_c=0$ we have the standard velocity profile with Navier slip. It should be noted that the no-slip case corresponds to $B\to 0$. The volumetric flow rate is given by

$$Q=\begin{cases}\frac{\pi R^4G}{8\eta}, & G\leqslant G_c,\\ \frac{\pi R^4(1+4B)G}{8\eta}-\frac{\tau_cB\pi R^3}{\eta}, & G>G_c.\end{cases} \tag{11}$$

Introducing the following non-dimensional quantities

$$u_z^*=\frac{u_z\eta}{\tau_cR},\quad G^*=\frac{RG}{\tau_c},\quad \tau^*=\frac{\tau}{\tau_c},\quad Q^*=\frac{Q\eta}{\pi\tau_cR^3},\quad r^*=\frac{r}{R}, \tag{12}$$

where the stars denote non-dimensional variables, the non-dimensional critical pressure gradient becomes $G_c^*=2$. The non-dimensional velocity and volumetric flow rate are respectively given by

$$u_z^*=\begin{cases}\frac{G^*(1-r^{*2})}{4}, & G^*\leqslant 2,\\ \frac{G^*(1+2B-r^{*2})}{4}-B, & G^*>2,\end{cases} \tag{13}$$

and

$$Q^*=\begin{cases}\frac{G^*}{8}, & G^*\leqslant 2,\\ \frac{(1+4B)G^*}{8}-B, & G^*>2.\end{cases} \tag{14}$$

The dimensionless volumetric flow rate Q^* for different values of the slip number is shown in Fig. 1. As deduced from Eq. (14), the first branch is independent of the slip number B. The slope of the second branch increases with B, ranging from 1/8 (no-slip) to infinity (full slip).

2.1. Plane Poiseuille flow

For completeness, we provide here the dimensionless solution for the plane Poiseuille flow. Using similar scales,

$$u_x^*=\frac{u_x\eta}{\tau_cH},\quad G^*=\frac{HG}{\tau_c},\quad \tau^*=\frac{\tau}{\tau_c},\quad Q^*=\frac{Q\eta}{\tau_cH^3},\quad y^*=\frac{y}{H}, \tag{15}$$

one finds that the critical pressure gradient for the occurrence of slip is $G_c^*=1$. The non-dimensional velocity is

$$u_x^*=\begin{cases}\frac{G^*(1-y^{*2})}{2}, & G^*\leqslant 1,\\ \frac{G^*(1+2B-y^{*2})}{2}-B, & G^*>1.\end{cases} \tag{16}$$

and the non-dimensional volumetric flow rate is

$$Q^*=\begin{cases}\frac{2G^*}{3}, & G^*\leqslant 1,\\ \frac{2(1+3B)G^*}{3}-B, & G^*>1,\end{cases} \tag{17}$$

where $B\equiv\eta/(\beta H)$ is the slip number.

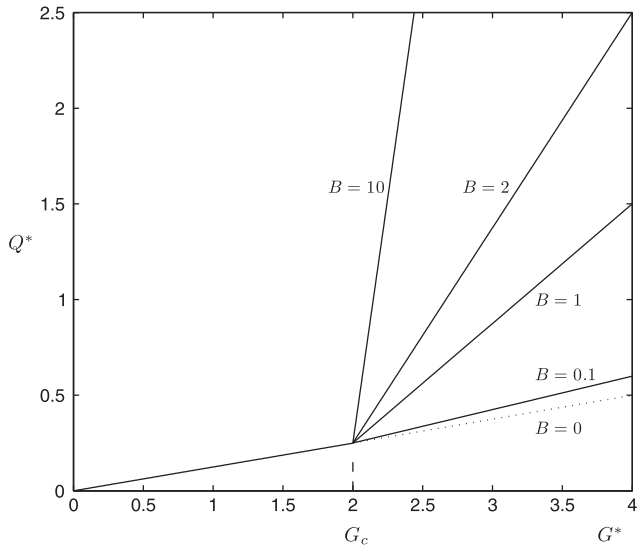

Fig. 1. The dimensionless volumetric flow rate Q^* in the axisymmetric case for various values of B.

3. Annular Poiseuille flow

Here, we consider the one-dimensional, steady problem for an annulus of radii kR, with $0 < k < 1$, assuming that the two walls are of the same properties (so that the same slip equation applies on both walls). Therefore, the axial velocity $u_z(r)$ is subject to the boundary conditions

$$u_{w1} = \begin{cases} 0, & \tau_{w1} \leqslant \tau_c, \\ -\frac{1}{\beta}\left(-\eta\frac{du_z}{dr} + \tau_c\right), & \tau_{w1} > \tau_c, \end{cases} \quad \text{on } r = kR, \tag{18}$$

$$u_{w2} = \begin{cases} 0, & \tau_{w2} \leqslant \tau_c, \\ -\frac{1}{\beta}\left(\eta\frac{du_z}{dr} + \tau_c\right), & \tau_{w2} > \tau_c, \end{cases} \quad \text{on } r = R, \tag{19}$$

where the subscripts 1 and 2 denote the quantities at $r = kR$ and $r = R$, respectively. It is easy to see that $\tau_{w1} > \tau_{w2}$ and hence as the pressure gradient is increased slip first occurs at the inner wall and then at the outer wall [16]. Thus, there are three flow regimes and two critical pressure gradients in this problem.

(i) No-slip

For $\tau_{wi} \leqslant \tau_c$, $i = 1, 2$ one gets the classical no-slip solution

$$u_z(r) = \frac{R^2 G}{4\eta}\left[1 - \left(\frac{r}{R}\right)^2 + \frac{1-k^2}{\ln(1/k)}\ln\frac{r}{R}\right], \tag{20}$$

with

$$Q = \frac{\pi R^4}{8\eta}\left[1 - k^4 - \frac{(1-k^2)^2}{\ln(1/k)}\right]G. \tag{21}$$

The two wall shear stresses are given by

$$\tau_{w1} = \frac{R}{4}\left[\frac{1-k^2}{k\ln(1/k)} - 2k\right]G, \quad \tau_{w2} = \frac{R}{4}\left[2 - \frac{1-k^2}{\ln(1/k)}\right]G. \tag{22}$$

Therefore, the first critical pressure gradient G_{c1} corresponds to $\tau_{w1} = \tau_c$,

$$G_{c1} = \frac{4k\ln(1/k)\tau_c}{[-2k^2\ln(1/k) + 1 - k^2]R}. \tag{23}$$

(ii) Slip only at the inner wall

Once the critical pressure gradient G_{c1} is exceeded $\tau_{w1} > \tau_c$ but in a certain range still $\tau_{w2} \leqslant \tau_c$. In other words, slip occurs only along the inner wall. One finds that

$$u_z(r) = \frac{R^2 G}{4\eta}\left[1 - \left(\frac{r}{R}\right)^2 + \frac{2Bk + 1 - k^2}{\ln(1/k) + B/k}\ln\frac{r}{R}\right] + \frac{\tau_c BR}{\eta} \times \frac{1}{\ln(1/k) + B/k}\ln\frac{r}{R}, \tag{24}$$

and

$$Q = \frac{\pi R^4}{8\eta}\left[1 - k^4 - \frac{(1-k^2)^2 - 4Bk[k^2\ln(1/k) - 1 + k^2]}{\ln(1/k) + B/k}\right]G + \frac{\pi\tau_c BR^3}{2\eta}\frac{[2k^2\ln(1/k) - 1 + k^2]}{\ln(1/k) + B/k}. \tag{25}$$

The wall shear stresses are now given by

$$\tau_{w1} = \frac{R}{4}\left[-2k + \frac{2Bk + 1 - k^2}{k[\ln(1/k) + B/k]}\right]G + \frac{\tau_c B}{k[\ln(1/k) + B/k]}, \tag{26}$$

and

$$\tau_{w2} = \frac{R}{4}\left[2 - \frac{2Bk + 1 - k^2}{\ln(1/k) + B/k}\right]G - \frac{\tau_c B}{\ln(1/k) + B/k}. \tag{27}$$

The second critical pressure gradient G_{c2} for the occurrence of slip at the outer wall corresponds to $\tau_{w2} = \tau_c$. Thus,

$$G_{c2} = \frac{4[\ln(1/k) + B(1 + 1/k)]\tau_c}{[2\ln(1/k) + 2B/k(1-k^2) - 1 + k^2]R}. \tag{28}$$

(iii) Slip at both walls

Once the second critical pressure gradient G_{c2} is exceeded, $\tau_{wi} > \tau_c$, $i = 1, 2$, and slip occurs along both walls. The velocity and the volumetric flow rate are given by

$$u_z(r) = \frac{R^2 G}{4\eta}\left[1 + 2B - \left(\frac{r}{R}\right)^2 + \frac{2B(1+k) + 1 - k^2}{\ln(1/k) + B(1 + 1/k)}\left(\ln\frac{r}{R} - B\right)\right] - \frac{\tau_c BR}{\eta}, \tag{29}$$

and

$$Q = \frac{\pi R^4}{8\eta}\left[1 - k^4 + 4B - \frac{(1 - k^2 + 2B)^2 - 4Bk[k^2\ln(1/k) - 1 + k^2 - 2B + Bk^2]}{\ln(1/k) + B(1 + 1/k)}\right]G - \frac{\pi\tau_c BR^3(1-k^2)}{\eta}. \tag{30}$$

In the special case where we have no slip setting $B = 0$ leads to the no-slip expression (20). The stress is given by

$$\tau_z(r) = \frac{G}{4}\left[-2r + \frac{2B(1+k) + 1 - k^2}{\ln(1/k) + B(1 + 1/k)}\frac{R^2}{r}\right]. \tag{31}$$

The two wall shear stresses are

$$\tau_{w1} = \frac{R}{4}\left[\frac{2B(1+k) + 1 - k^2}{k[\ln(1/k) + B(1 + 1/k)]} - 2k\right]G,$$

$$\tau_{w2} = \frac{R}{4}\left[2 - \frac{2B(1+k) + 1 - k^2}{\ln(1/k) + B(1 + 1/k)}\right]G. \tag{32}$$

Using the non-dimensional variables in (12) gives the two non-dimensional critical pressure gradients

$$G^*_{c1} = \frac{4k\ln(1/k)}{-2k^2\ln(1/k) + 1 - k^2},$$

$$G^*_{c2} = \frac{4[\ln(1/k) + B + B/k]}{2\ln(1/k) + 2B(1-k^2)/k - 1 + k^2}. \tag{33}$$

The non-dimensional velocity is

$$u^*_z(r) = \begin{cases} \frac{G^*}{4}\left[1 - r^{*2} + \frac{1-k^2}{\ln(1/k)}\ln r^*\right], & G^* \leqslant G^*_{c1}, \\ \frac{G^*}{4}\left[1 - r^{*2} + \frac{2Bk+1-k^2}{\ln(1/k)+B/k}\ln r^*\right] + \frac{B}{\ln(1/k)+B/k}\ln r^*, & G^*_{c1} < G^* \leqslant G^*_{c2}, \\ \frac{G^*}{4}\left[1 + 2B - r^{*2} + \frac{2B(1+k)+1-k^2}{\ln(1/k)+B(1+1/k)}(\ln r^* - B)\right] - B, & G^* > G^*_{c2}. \end{cases} \tag{34}$$

The non-dimensional volumetric flow rate is given by

$$Q^* = \begin{cases} \frac{1}{8}\left[(1-k^4) - \frac{(1-k^2)^2}{\ln(1/k)}\right]G^*, & G^* \leqslant G^*_{c1}, \\ \frac{1}{8}\left[(1-k^4) - \frac{(1-k^2)^2 - N_1}{\ln(1/k)+B/k}\right]G^* + \frac{B}{2}\frac{[2k^2\ln(1/k) - 1 + k^2]}{\ln(1/k)+B/k}, & G^*_{c1} < G^* \leqslant G^*_{c2}, \\ \frac{1}{4}\left[1 - k^4 + 4B - \frac{(1-k^2+2B)^2 - N_2}{\ln(1/k)+B(1+1/k)}\right]G^* - B(1-k^2), & G^* > G^*_{c2}, \end{cases} \tag{35}$$

where $N_1 \equiv 4Bk[k^2\ln(1/k) - 1 + k^2]$ and $N_2 \equiv 4Bk[k^2\ln(1/k) - 1 + k^2 - 2B + Bk^2]$. Fig. 2 shows the dimensionless velocity profiles for $k = 0.1$ and $B = 1$ at various pressure gradients including the two critical values separating the three flow regimes. It should be noted that at very high pressure gradients the velocity profile tends to become uniform (full slip). In Fig. 3 the non-dimensional volumetric flow rate is shown for $k = 0.1$ and three slip numbers ($B = 0.1$, 1, and 10). As indicated by Eq. (33), while the first branch and G_{c1} are independent of B, G_{c2} is decreased reduced as B is increased and the slopes of the last two branches increase as B is increased. For the two slip velocities one gets

$$u^*_{w1} = \begin{cases} 0, & G^* \leqslant G^*_{c1}, \\ \frac{1}{4}\left[1 - k^2 - \frac{(2Bk+1-k^2)\ln(1/k)}{\ln(1/k)+B/k}\right]G^* - \frac{B\ln(1/k)}{\ln(1/k)+B/k}, & G^*_{c1} < G^* \leqslant G^*_{c2}, \\ \frac{1}{4}\left[1 + 2B - k^2 - \frac{2B(1+k)+1-k^2}{\ln(1/k)+B(1+1/k)}[\ln(1/k)+B]\right]G^* - B, & G^* > G^*_{c2}, \end{cases} \tag{36}$$

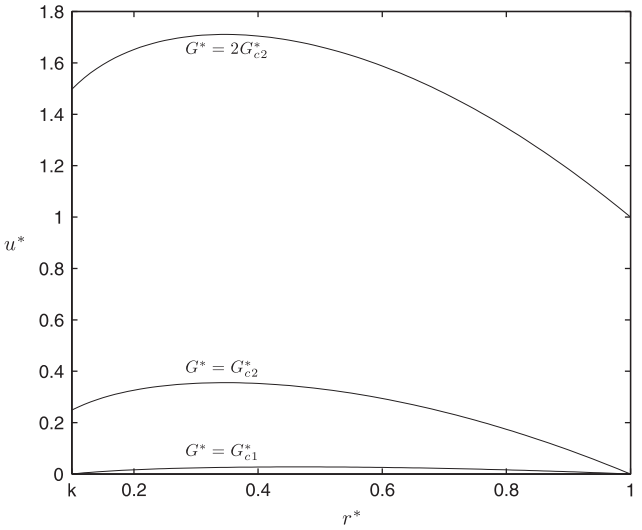

Fig. 2. The velocity profile u^* in annular Poiseuille flow for $k = 0.1$, $B = 1$ and various values of the pressure gradient.

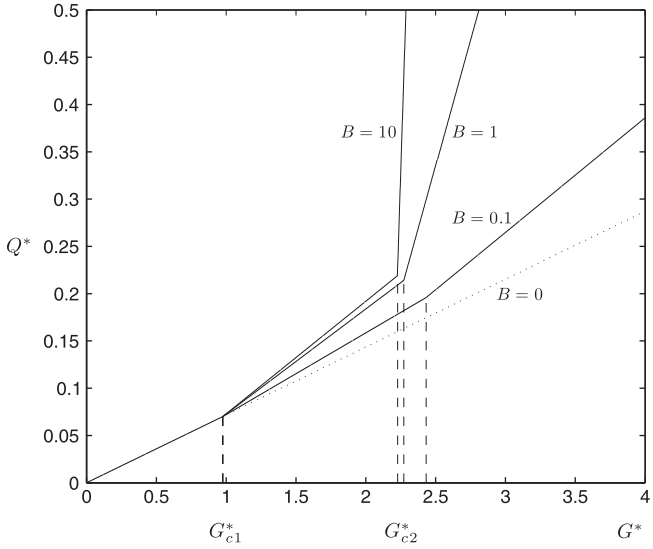

Fig. 3. The volumetric flow rate Q^* in annular Poiseuille flow with $k = 0.1$ for various slip numbers.

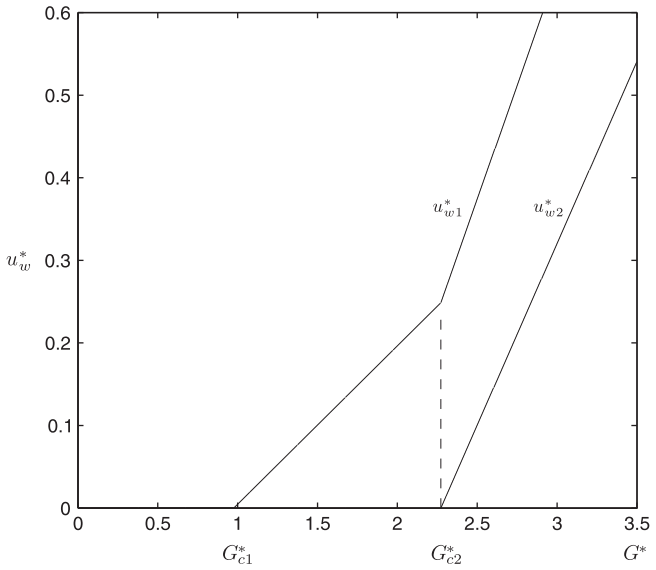

Fig. 4. The wall velocities u^*_w in annular Poiseuille flow with $k = 0.1$ and $B = 1$.

$$u^*_{w2} = \begin{cases} 0, & G^* \leqslant G^*_{c2}, \\ \frac{1}{4}\left[2B - \frac{2B(1+k)+1-k^2}{\ln(1/k)+B(1+1/k)}B\right]G^* - B, & G^* > G^*_{c2}. \end{cases} \tag{37}$$

Fig. 4 shows the variation of the two slip velocities as the dimensionless pressure gradient is increased for $k = 0.1$ and $B = 1$.

In the case where the two walls are made of different properties the critical yield stress and the slip number are different at each wall. The flow regimes are again three, however slip may occur first at the outer wall. The solution to this more general flow is summarised in the Appendix A.

4. Rectangular Poiseuille flow

We now consider, the steady Poiseuille flow in a tube of rectangular cross-section with $-b \leqslant y \leqslant b$, $-c \leqslant z \leqslant c$, where $b \geqslant c$. This flow is governed by the two-dimensional Poisson's equation

$$\frac{\partial^2 u_x}{\partial y^2} + \frac{\partial^2 u_x}{\partial z^2} = -\frac{G}{\eta}. \tag{38}$$

Assuming that slip with non-zero slip yield stress occurs at the walls, which share the same properties, the boundary conditions of the flow are

$$u_w = \begin{cases} 0, & \tau_w \leqslant \tau_c, \\ -\frac{1}{\beta}\left(\eta\frac{\partial u_x}{\partial y} + \tau_c\right) & \tau_w > \tau_c, \end{cases} \qquad \text{on } y = \pm b,\ -c \leqslant z \leqslant c, \tag{39}$$

$$u_w = \begin{cases} 0, & \tau_w \leqslant \tau_c, \\ -\frac{1}{\beta}\left(\eta\frac{\partial u_x}{\partial z} + \tau_c\right) & \tau_w > \tau_c, \end{cases} \qquad \text{on } z = \pm c,\ -b \leqslant y \leqslant b. \tag{40}$$

4.1. The no-slip regime

The classical no-slip solution [13] is

$$u_x(y,z) = \frac{2Gc^2}{\eta}\sum_{k=1}^{\infty}\frac{(-1)^{k+1}}{\lambda_k^3}\cos(z\lambda_k/c)\left[1 - \frac{\cosh(y\lambda_k/c)}{\cosh(b\lambda_k/c)}\right], \tag{41}$$

and the volumetric flow rate is given by

$$Q = \frac{8Gbc^3}{\eta}\sum_{k=1}^{\infty}\frac{1}{\lambda_k^4}\left[\lambda_k - \frac{c\tanh(b\lambda_k/c)}{b}\right], \tag{42}$$

where $\lambda_k = (2k-1)/2\pi$, $k = 1,2,\ldots$. The wall shear stresses along walls $y = b$ and $z = c$ are respectively

$$\tau_{wy}(z) = 2cG\sum_{k=1}^{\infty}\frac{(-1)^{k+1}}{\lambda_k^2}\tanh(b\lambda_k/c)\cos(z\lambda_k/c), \tag{43}$$

$$\tau_{wz}(y) = 2cG\sum_{k=1}^{\infty}\frac{1}{\lambda_k^2}\left[1-\frac{\cosh(y\lambda_k/c)}{\cosh(b\lambda_k/c)}\right]. \tag{44}$$

The maximum stresses occur at the middle of each side of the rectangular duct: $\tau_{wy,max} = \tau_{wy}(0)$, $\tau_{wz,max} = \tau_{wz}(0)$. It can be seen that $\tau_{wz,max} \geqslant \tau_{wy,max}$, thus slip occurs first at the wider wall ($z = c$). Hence, the critical pressure gradient below which no slip occurs corresponds to $\tau_{wz,max} = \tau_c$ and is given by

$$G_{c1} = \frac{\tau_c}{2c\sum_{k=1}^{\infty}\frac{1}{\lambda_k^2}[1-\operatorname{sech}(b\lambda_k/c)]}. \tag{45}$$

Once the critical pressure gradient is exceeded, slip occurs only at the middle of the wider walls. As the pressure gradient is increased, slip eventually occurs in the middle of the narrower walls as illustrated in Fig. 5. It is only at a certain critical value of the pressure gradient that non-uniform slip occurs everywhere along all walls. When slip along the walls is partial the problem is not amenable to analytical solution.

4.2. The solution in the case of "full" slip

The full slip solution is given by

$$u_x(y,z) = \frac{2c^2G}{\eta}\sum_{k=1}^{\infty}\frac{\cos(z\lambda_k/c)\sin\lambda_k}{\lambda_k^2(\lambda_k+\sin\lambda_k\cos\lambda_k)} \times\left[1-\frac{\cosh(y\lambda_k/c)}{\cosh(b\lambda_k/c)+B\lambda_k\sinh(b\lambda_k/c)}\right]-\frac{\tau_cBc}{\eta} \tag{46}$$

where

$$B \equiv \frac{\eta}{\beta c} \tag{47}$$

and λ_k, $k = 1,2,\ldots$, are the roots of

$$\lambda_k\tan\lambda_k = \frac{1}{B}. \tag{48}$$

The wall shear stresses along $y = b$ and $z = c$ are respectively,

$$\tau_{wy}(z) = 2cG\sum_{k=1}^{\infty}\left[\frac{\sinh(b\lambda_k/c)}{\cosh(b\lambda_k/c)+B\lambda_k\sinh(b\lambda_k/c)}\right]\frac{\sin\lambda_k\cos(z\lambda_k/c)}{\lambda_k(\lambda_k+\sin\lambda_k\cos\lambda_k)}, \tag{49}$$

and

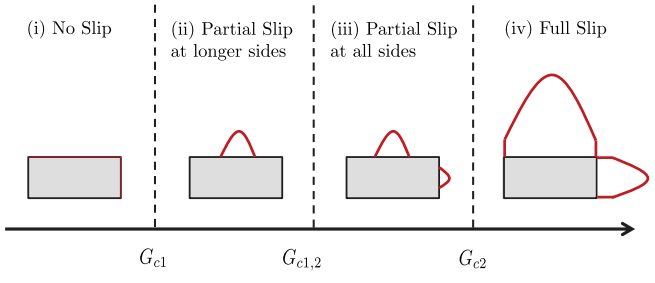

Fig. 5. Sketch (not drawn to scale) showing the various flow regimes for the rectangular problem in the case of non-zero slip yield stress. Here, $b > c$.

$$\tau_{wz}(y) = 2cG\sum_{k=1}^{\infty}\frac{\sin^2\lambda_k}{\lambda_k(\lambda_k+\sin\lambda_k\cos\lambda_k)} \times\left[1-\frac{\cosh(y\lambda_k/c)}{\cosh(b\lambda_k/c)+B\lambda_k\sinh(b\lambda_k/c)}\right]. \tag{50}$$

The maximum stresses at each wall are now given by $\tau_{wy,max} = -\tau_{wy}(0)$, $\tau_{wz,max} = \tau_{wz}(0)$, and the minimum stress occurs at the corners of the rectangular duct: $\tau_{wy,min} = \tau_{wy}(c)$, $\tau_{wz,min} = \tau_{wz}(b)$. If $\tau_{wz,min} \leqslant \tau_c < \tau_{wz,max}$ and $\tau_{wy,max} \leqslant \tau_c$ slip does occur but only in the central part of the wider sides (see (ii) in Fig. 5) and if $\{\tau_{wy,min}, -\tau_{wz,min}\} \leqslant \tau_c < \tau_{wy,max}$ slip does occur but only in the central parts of all walls (see (iii) in Fig. 5). If $\tau_{wy,min} > \tau_c$ slip occurs everywhere on all walls and the corresponding critical pressure gradient is

$$G_{c2} = \frac{\tau_c}{2c\sum_{k=1}^{\infty}\frac{\sin^2\lambda_k}{\lambda_k(\lambda_k+\sin\lambda_k\cos\lambda_k)}\left[1-\frac{1}{1+B\lambda_k\tanh(b\lambda_k/c)}\right]}. \tag{51}$$

The volumetric flow rate is given by

$$Q = \frac{8bc^3G}{\eta}\sum_{k=1}^{\infty}\frac{\sin^2\lambda_k}{\lambda_k^4(\lambda_k+\sin\lambda_k\cos\lambda_k)} \times\left[\lambda_k-\frac{c}{b}\frac{\sinh(b\lambda_k/c)}{\cosh b\lambda_k/c+B\lambda_k\sinh b\lambda_k/c}\right]-\frac{4\tau_cBbc^2}{\eta}. \tag{52}$$

Introducing the scalings

$$u^* = \frac{u_x\eta}{\tau_cc}, \quad G^* = \frac{cG}{\tau_c}, \quad Q^* = \frac{Q\eta}{\tau_cbc^2} \quad z^* = \frac{z}{c}, \quad y^* = \frac{y}{b}, \quad \alpha = \frac{c}{b}, \tag{53}$$

gives the following expressions for the non-dimensional critical pressure gradients

$$G_{c1}^* = \frac{1}{2\sum_{k=1}^{\infty}\frac{1}{\lambda_k^2}[1-\operatorname{sech}(\lambda_k/\alpha)]}, \tag{54}$$

and

$$G_{c2}^* = \frac{1}{2\sum_{k=1}^{\infty}\frac{\sin^2\lambda_k}{\lambda_k(\lambda_k+\sin\lambda_k\cos\lambda_k)}\left[1-\frac{1}{1+B\lambda_k\tanh(\lambda_k/\alpha)}\right]}. \tag{55}$$

The non-dimensional velocity is

$$u^* = \begin{cases} 2G^*\sum_{k=1}^{\infty}\frac{(-1)^{k+1}}{\lambda_k^2}\cos(z^*\lambda_k)\left[1-\frac{\cosh(y^*\lambda_k/\alpha)}{\cosh(\lambda_k/\alpha)}\right], & G^* \leqslant G_{c1}^*, \\ 2G^*\sum_{k=1}^{\infty}\frac{\sin\lambda_k\cos(z^*\lambda_k)}{\lambda_k^2(\lambda_k+\sin\lambda_k\cos\lambda_k)}\left[1-\frac{\cosh(y^*\lambda_k/\alpha)}{\cosh(\lambda_k/\alpha)+B\lambda_k\sinh(\lambda_k/\alpha)}\right]-B, & G^* > G_{c2}^*, \end{cases} \tag{56}$$

and the non-dimensional volumetric flow rate

$$Q^* = \begin{cases} 8G^*\sum_{k=1}^{\infty}\frac{\lambda_k-\alpha\tanh\lambda_k/\alpha}{\lambda_k^4}, & G^* \leqslant G_{c1}^*, \\ 8G^*\sum_{k=1}^{\infty}\frac{\sin^2\lambda_k}{\lambda_k^4(\lambda_k+\sin\lambda_k\cos\lambda_k)}\left[\lambda_k-\frac{\alpha\sinh\lambda_k/\alpha}{\cosh(\lambda_k/\alpha+B\lambda_k)\sinh(\lambda_k/\alpha)}\right]-4B, & G^* > G_{c2}^*. \end{cases} \tag{57}$$

The non-dimensional volumetric flow rate as a function of the pressure gradient is shown in Fig. 6 for different slip numbers. The lower branch corresponds to the no-slip flow regime. The upper-branch corresponding to the "full" slip case has a higher slope depending on the slip number B. The dashed lines in the region between the dotted lines correspond to partial slip cases (ii) and (iii) for which there are no analytical solutions.

Finally, in Fig. 7 the velocity contours at different values of the dimensionless pressure gradient are shown for $B = 1$. It should be

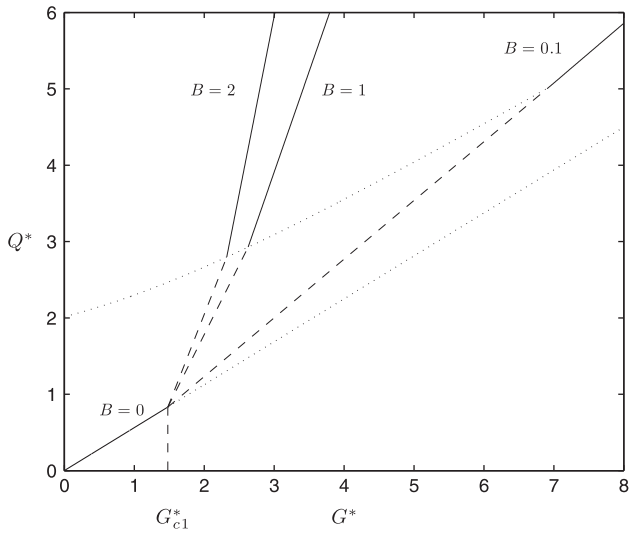

Fig. 6. The volumetric flow rate Q^* for the rectangular problem is plotted against the pressure gradient for various values of B and arbitrary τ_c. The region between the dotted lines, corresponds to the intermediate regimes (ii) and (iii) for which there are no analytical solutions.

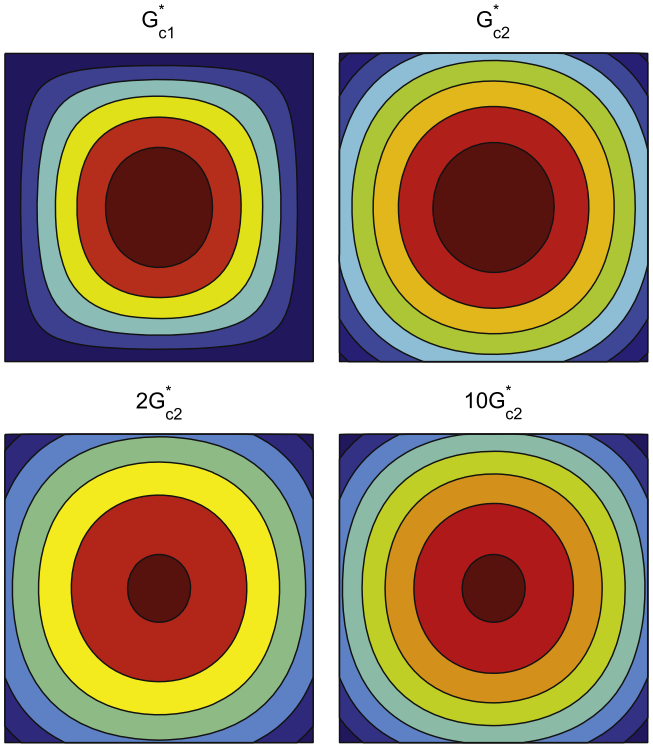

Fig. 7. Velocity contours for $B = 1$ and different values of the dimensionless pressure gradient.

noted that the magnitude of the velocity increases with pressure gradient.

5. Conclusions

We have derived analytical solutions for the steady, incompressible Newtonian Poiseuille flow in various geometries assuming that slip occurs along the wall, following a Navier-type slip law with a non-zero slip yield stress. For the axisymmetric problem there are two distinct flow regimes corresponding to no-slip and slip, defined by a critical value of the imposed pressure gradient, which depends solely on the slip yield stress.

The annular problem is more complicated with three distinct flow regimes defined by two critical values of the pressure gradient corresponding to the triggering of slip at the inner and outer walls of the annulus. The first depends solely on the slip yield stress while the second critical value also depends on the slip coefficient.

In the rectangular Poiseuille flow case, below a first critical pressure gradient there is no-slip and above a second critical value, non-uniform slip occurs everywhere along the walls. Between these two critical pressure gradients there are two intermediate flow regimes, for which there are no analytical solutions. In the first intermediate regime there is only partial slip along the middle section of the wider walls. In the second intermediate regime partial slip along the middle sections of the narrower walls is observed. (In the special case of a square cross-section there is only one intermediate flow regime). The numerical solution of the flow in these intermediate regimes and other geometries are the subject of our current investigations.

Appendix A

Here, we consider the case where the two walls in annular Poiseuille flow are of different properties so that the boundary conditions read:

$$u_{w1} = \begin{cases} 0, & \tau_{w1} \leqslant \tau_{c1}, \\ -\frac{1}{\beta_1}\left(-\eta \frac{du_z}{dr} + \tau_{c1}\right), & \tau_{w1} > \tau_{c1}, \end{cases} \quad \text{on } r = kR, \tag{A.1}$$

$$u_{w2} = \begin{cases} 0, & \tau_{w2} \leqslant \tau_{c2}, \\ -\frac{1}{\beta_2}\left(\eta \frac{du_z}{dr} + \tau_{c2}\right), & \tau_{w2} > \tau_{c2}, \end{cases} \quad \text{on } r = R. \tag{A.2}$$

Obviously the solution in the no-slip regime is that given by Eqs. (20)–(22). Depending on the values of the slip parameters β_1 and β_2 and the slip yield stresses τ_{c1} and τ_{c2}, for the two walls, slip may occur first in either wall. The first critical pressure gradient for the occurrence of slip is

$$G_{c1} = \frac{4\ln(1/k)}{R} \times \min\left\{\frac{k\tau_{c1}}{-2k^2\ln(1/k) + 1 - k^2}, \frac{\tau_{c2}}{2\ln(1/k) - 1 + k^2}\right\}. \tag{A.3}$$

If slip occurs first at the inner wall the velocity is given by

$$u_z(r) = \frac{R^2 G}{4\eta}\left[1 - \left(\frac{r}{R}\right)^2 + \frac{2B_1 k + 1 - k^2}{\ln(1/k) + B_1/k}\ln\frac{r}{R}\right] + \frac{\tau_{c1}B_1 R}{\eta} \times \frac{1}{\ln(1/k) + B_1/k}\ln\frac{r}{R}; \tag{A.4}$$

otherwise

$$u_z(r) = \frac{R^2 G}{4\eta}\left[1 + 2B_2 - \left(\frac{r}{R}\right)^2 + \frac{2B_2 + 1 - k^2}{\ln(1/k) + B_2}\left(\ln\frac{r}{R} - B_2\right)\right] - \frac{\tau_{c2}B_2 R}{\eta} - \frac{\tau_{c2}B_2 R}{\eta}\frac{1}{\ln(1/k) + B_2}\left(\ln\frac{r}{R} - B_2\right), \tag{A.5}$$

where B_i, $i = 1, 2$ are the dimensionless slip numbers at each wall defined by $B_i \equiv \eta/(\beta_i R)$, $i = 1, 2$. The second critical pressure gradient for the occurrence of slip at the other wall is

$$G_{c2} = \frac{4}{R}\min\left\{\frac{\tau_{c2}(\ln(1/k)+B_1/k)+\tau_{c1}B_1}{2\ln(1/k)+2B/k(1-k^2)-1+k^2}, \frac{\tau_{c1}k(\ln(1/k)+B_2)-\tau_{c2}B_2}{-2k^2\ln(1/k)+2B(1-k^2)+1-k^2}\right\}. \quad (A.6)$$

Therefore, for $G > G_{c2}$ slip occurs at both walls and the velocity is given by

$$u_z(r) = \frac{R^2G}{4\eta}\left[1+2B_2-\left(\frac{r}{R}\right)^2+\frac{2(B_1k+B_2)+1-k^2}{\ln(1/k)+B_2+B_1/k}\left(\ln\frac{r}{R}-B_2\right)\right] - \frac{\tau_{c2}B_2R}{\eta}+\frac{R}{\eta}\frac{(\tau_{c1}B_1-\tau_{c2}B_2)}{[\ln(1/k)+B_2+B_1/k]}\left(\ln\frac{r}{R}-B_2\right). \quad (A.7)$$

The wall shear stresses are given by

$$\tau_{w1} = \frac{R}{4}\left[\frac{L(B_1,B_2)}{k}-2k\right]G-\frac{M}{k}, \quad \tau_{w2} = \frac{R}{4}[2-L(B_1,B_2)]G+M, \quad (A.8)$$

where

$$L(B_1,B_2) = \frac{2(B_1k+B_2)+1-k^2}{\ln(1/k)+B_2+B_1/k}, \quad M(B_1,B_2) = \frac{\tau_{c1}B_1-\tau_{c2}B_2}{\ln(1/k)+B_2+B_1/k} \quad (A.9)$$

Finally, the volumetric flow rate is

$$Q = \frac{\pi R^4}{8\eta}\left[1-k^2+4B_2 - \frac{(1-k^2-2B_2)^2-4B_1k[k^2\ln(1/k)-1+k^2-2B_2+B_2k^2]}{\ln(1/k)+B_2+B_1/k}\right]G - \frac{\pi\tau_{c2}B_2R^3}{\eta}+\frac{\pi R^3M}{2\eta}\left[2k^2\ln(1/k)-(1-k^2)(1+2B_2)\right]. \quad (A.10)$$

References

[1] H.A. Barnes, A review of the slip (wall depletion) of polymer solutions, emulsions and particle suspensions in viscometers: its cause, character, and cure, J. Non-Newton. Fluid Mech. 56 (1995) 221–251.

[2] M.M. Denn, Extrusion instabilities and wall slip, Ann. Rev. Fluid Mech. 33 (2001) 265–287.

[3] S.G. Hatzikiriakos, Wall slip of molten polymers, Prog. Polym. Sci. 37 (2012) 624–643.

[4] C. Neto, D.R. Evans, E. Bonaccurso, H.J. Butt, V.S.J. Craig, Boundary slip in Newtonian liquids: a review of experimental studies, Rep. Prog. Phys. 68 (2005) 2859–2897.

[5] E.B. Arkilic, M.A. Schmidt, K.S. Breuer, Gaseous slip flow in long microchannels, J. Microelectromech. Syst. 6 (1997) 167–178.

[6] J. Liu, Y.C. Tai, C.M. Ho, MEMS for pressure distribution studies of gaseous flows in microchannels, in: IEEE International Conference on Micro Electro Mechanical Systems, Amsterdam, Netherlands, 1995, pp. 209–215.

[7] T. Araki, M.S. Kim, I. Hiroshi, K. Suzuki, An experimental investigation of gaseous flow characteristics in microchannels, in: G.P. Celata, V.P. Carey, M. Groll, I. Tanasawa, G. Zummo (Eds.), Proceedings of International Conference on Heat Transfer and Transport Phenomena in Microscale, Begell House, New York, 2000, pp. 155–161.

[8] C.L.M.H. Navier, Sur les lois de mouvement des fluides, Mem. Acad. R. Sci. Inst. Fr. 6 (1827) 289–440.

[9] M.T. Matthews, J.M. Hill, Nanofluidics and the Navier boundary condition, Int. J. Nanotechnol. 5 (2008) 218–242.

[10] Y. Damianou, G.C. Georgiou, I. Moulitsas, Combined effects of compressibility and slip in flows of a Herschel?Bulkley fluid, J. Non-Newton. Fluid Mech. 193 (2013) 89–102.

[11] P. Estellè, C. Lanos, Squeeze flow of Bingham fluids under slip with friction boundary condition, Rheol. Acta 46 (2007) 397–404.

[12] P. Ballesta, G. Petekidis, L. Isa, W.C.K. Poon, R. Besseling, Wall slip and flow of concentrated hard-sphere colloidal suspensions, J. Rheol. 56 (2012) 1005–1037.

[13] W.A. Ebert, E.M. Sparrow, Slip flow in rectangular and annular ducts, J. Basic Eng. 87 (1965) 1018–1024.

[14] Z. Duan, Y. Muzychka, Slip flow in non-circular microchannels, Microfluid. Nanofluid. 3 (2007) 473–484.

[15] Z. Duan, Y.S. Muzychka, Slip flow in elliptic microchannels, Int. J. Therm. Sci. 46 (2007) 1104–1111.

[16] M. Chatzimina, G.C. Georgiou, K. Housiadas, S.G. Hatzikiriakos, Stability of the annular Poiseuille flow of a Newtonian liquid with slip along the walls, J. Non-Newton. Fluid Mech. 159 (2009) 1–9.

[17] Y.H. Wu, B. Wiwatanapataphee, M. Hu, Pressure-driven transient flows of Newtonian fluids through microtubes with slip boundary, Phys. A: Stat. Mech. Appl. 387 (2008) 5979–5990.

[18] B. Wiwatanapataphee, Y.H. Wu, M. Hu, K. Chayantrakom, A study of transient flows of Newtonian fluids through micro-annuals with a slip boundary, J. Phys. A: Math. Theor. 42 (2009) 065206.

[19] X. He, D.N. Ku, J.E. Moore, Simple calculation of the velocity profiles for pulsatile flow in a blood vessel using mathematica, Ann. Biomed. Eng. 21 (1993) 45–49.

[20] M.R. King, Oscillatory gas flow in a circular nanotube, Open Nanosci. J. 1 (2007) 1–4.

[21] J. Majdalani, Exact Navier-Stokes solution for pulsatory viscous channel flow with arbitrary pressure gradient, J. Propul. Power 24 (2008) 1412–1423.

[22] L.L. Ferrás, J.M. Nóbrega, F.T. Pinho, Analytical solutions for Newtonian and inelastic non-Newtonian flows with wall slip, J. Non-Newton. Fluid Mech. 175–176 (2012) 76–88.